Tracking attention using RIFT with a consumer-monitor setup

Ü. Gülce Çelik*, Kabir Arora*, J. Leon Kenemans, Stefan Van der Stigchel,
Surya Gayet[†], Samson Chota[†]
Helmholtz Institute, Utrecht University, Heidelberglaan 1, 3584CS Utrecht, the Netherlands

*These authors contributed equally †These authors contributed equally

Abstract

Rapid Invisible Frequency Tagging (RIFT) is a recent technique that extends the traditional frequency tagging approach by stimulating at frequencies beyond the threshold of perception (≥60Hz). By doing so, it offers a measure of early visual processing without the confounding effect of introducing visible stimuli. This ability is most frequently harnessed as a tracker of covert attention in experimental paradigms across various disciplines in cognitive neuroscience. However, almost all existing RIFT work so far has made use of expensive display hardware limited in its accessibility. Recent work has successfully measured a RIFT response in combination with a 480Hz refresh consumer monitor, but it is not yet clear whether this setup can be utilized to track the locus of attention. Using a spatial cueing paradigm (n=24) while simultaneously tagging two locations (60Hz and 65.5Hz) on a 360Hz refresh rate monitor, we show that attentional modulations of early visual processing can be reliably measured with RIFT on a consumer monitor. We hope that this study will facilitate the widespread application of using consumer-grade high-refresh-rate gaming monitors with RIFT for future research.

Introduction

Frequency tagging is a common stimulation technique where different stimuli are flickered at unique frequencies, and the neural response to these can later be disentangled and uniquely tracked over time. Recent advancements in display technology have led to the emergence of a novel approach to frequency tagging known as Rapid Invisible Frequency Tagging (RIFT) (Zhigalov et al., 2019). Unlike traditional Steady-State Visual Evoked Potential (SSVEP) approaches that use slower flicker frequencies (<30Hz) which can be consciously perceived, RIFT employs a form of rapid stimulation using luminance flickers at frequencies beyond the threshold of perceptibility (\geq 60Hz). RIFT therefore offers a measure of early visual processing at specific locations in the visual field without the involvement of downstream visual processing regions associated with conscious perception (Zhigalov et al., 2019; Drijvers et al., 2021; Seijdel et al.,

2023; Arora et al., 2025). RIFT is most frequently utilized as a continuous and "invisible" tracker of spatial attention, measuring how attention influences cortical responses to specific locations in the visual field without (or before) presenting a perceptible stimulus (Zhigalov et al., 2019; Bouwkamp et al., 2025; Arora et al., 2024, 2025).

To date, most RIFT studies have utilized the PROPixx DLP-LED projector for the projection of stimuli on the screen to achieve the high refresh rate required for high-contrast luminance modulation. However, such specialized high-quality projection systems are often prohibitively expensive, which limits their accessibility to research groups. Moreover, the complexity of the setup of such display equipment can further restrict its availability to research laboratories. Conveniently, some recent consumer-grade (gaming) monitors are also able to reach high refresh rates similar to those that have been used with the PROPixx. Since these monitors are available at only a small fraction of the PROPixx's price, they offer a substantial reduction in hardware costs and provide a cost-effective alternative for conducting RIFT research.

Dimigen et al. (2025) recently utilized a commercially available 480 Hz organic light-emitting diode (OLED) monitor in combination with EEG and showed that such consumer-grade monitors can reliably deliver 480 Hz RIFT stimulation with accurate frame timings, with only rare single missed frames that do not seem to impact visibility (Dimigen et al., 2025). This study demonstrates the presence of a reliable RIFT response at two location conditions (i.e., central and peripheral). However, since this study did not incorporate an attentional manipulation, the essential question of whether RIFT responses measured with such monitors are sensitive to attentional modulations during cognitive experiments remains unanswered. Furthermore, they found that the tagging response from a peripheral stimulus was considerably weaker than that of a central stimulus, leaving open the question of whether tagging responses from peripheral stimuli – as are common in experiments on visuospatial attention – are sensitive enough to measure modulations of the RIFT response by attention even on a monitor setup.

This project builds on Dimigen et al. (2025) by including a spatial cueing task (to manipulate the allocation of attention) and tagging a larger set of locations in more participants. We had two main aims. Firstly, we utilized an off-the-shelf consumer-grade monitor (i.e., Alienware 500Hz Gaming Monitor AW2524HF) at a refresh rate of 360Hz and aimed to show that a robust RIFT response can be elicited using this novel display setup. Secondly, we examined whether the setup is sensitive enough to capture attentional modulations of the RIFT response across the visual field. To this end, we employed a cueing paradigm in 24 participants to investigate the deployment of covert spatial attention using RIFT in combination with EEG. Specifically, we tested whether a robust RIFT signal could be evoked using a consumer-grade gaming monitor at 360Hz, and crucially whether this would allow us to measure covert attentional modulations across the visual field. We believe that this would mark a key step toward making RIFT research more accessible and broadly applicable to the field of cognitive neuroscience.

Methods

Participants

We recruited 24 healthy participants (17 female, mean = 22.50 ± 1.69 years) with normal or corrected-to-normal vision. None of the participants reported a history of epilepsy or psychiatric diagnosis. Participants received compensation of either $\[\in \]$ 20 or a corresponding amount of participation credits in line with Utrecht University's internal participation framework (SONA). The study was conducted in accordance with the protocol approved by the Ethics Committee of the Faculty of Social and Behavioral Sciences at Utrecht University with reference number 863732 – HOMEOSTASIS (approved on 18/03/2020).

Experimental Design and Procedure

Participants reported the orientation of a target presented at one of eight locations as indicated by a spatial cue (**Figure 1**). The task presented eight identical circles arranged around a central fixation cross in two concentric rings: an inner ring of four circles and an outer ring of four circles positioned further away. The circles served as placeholder target/distractor locations. At each trial, a diagonally presented pair of circles was selected, with one circle tagged at 60Hz and the other at 65.45Hz (See **Tagging Manipulation**).

First, only the fixation cross was presented for a variable duration of 1000-1150 ms, followed by the eight circles on display, with a diametrically opposite pair of circles flickering at 60 and 65.45Hz (0.75 s). This was followed by an arrow cue (0.10s) that pointed to one of the two tagged circles, informing participants which location will be randomly cued on that trial. The size of the arrow cue was used to disambiguate between the near (smaller arrow cue) and far (larger arrow cue) circles in each diagonal direction, as the grid layout positions one circle at each eccentricity along every arrow direction. The cue was followed by a randomly uniform stimulus delay interval (0.75-1.0 s), after which two Landolt-C stimuli were displayed: one at the cued location (the target) and one at the diametrically opposite location at equal eccentricity (the distractor). Both locations were tagged. Participants were instructed to report the location of the aperture within the target Landolt-C (i.e., its orientation), which could be facing right, left, up, or down (responses were provided with the corresponding arrow key). The tagging of the (cued and uncued) circles was maintained until the end of the response period. Participants could respond up to 2.0s after the target onset. If no response was provided within this window, or if an incorrect button was pressed, the trial ended and participants were shown "incorrect" feedback (centrally presented). If the correct key was pressed, participants were shown 'correct' feedback. Each participant completed 900 trials (15 blocks of 60 trials each). The pair of circles that was tagged

(4 possible pairs), the target location (2 possible locations within each pair), and the orientation of the target stimulus (4 possible orientations) were presented equally often (individually, not counterbalanced) and in a different random order for each participant.

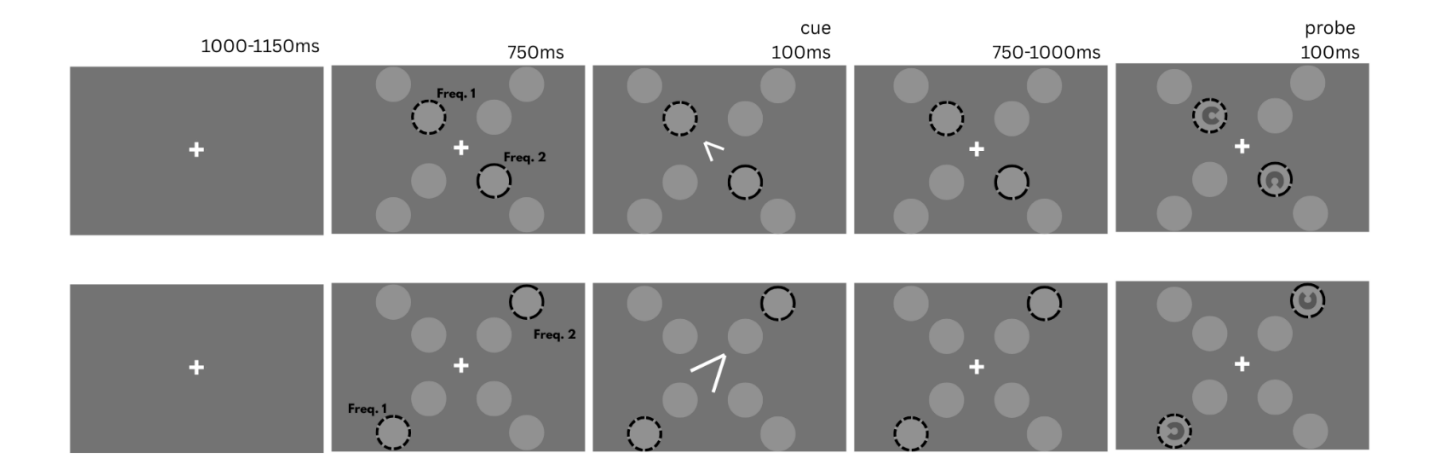


Figure 2.1: Task design. Participants reported the orientation of a target presented at one of eight locations as indicated by a spatial cue. Eight circles were presented around fixation, and a diagonally placed pair of circles was tagged. An arrow cue specified which of the eight locations the target will appear at. **Top:** This cue was either small, indicating that the near circle was cued, or **Bottom:** large, indicating that the far circle was cued. The target and the distractor were presented at the tagged locations. Participants indicated the orientation of the target (facing left, right, up, or down). The highlighted locations were flickered at 60 and 65.45Hz (see **Tagging Manipulation**) throughout the trial (not to scale).

Stimuli

The screen background was kept at the same dark grey color throughout the experiment (i.e., [60, 64, 61]), visibly darker than the tagged stimulus regions. Inner circles were positioned at a diagonal eccentricity of 4.5 dva, and outer circles at 8.1 dva, both offset equally in the horizontal and vertical directions from fixation. All circles were identical in size (r = 2.5 dva) and visual appearance. A white fixation cross composed of two perpendicular white lines (length = 0.65 dva, line width = 0.11 dva) was present in the center of the screen on each trial. The fixation cross stayed on the screen except for when it was replaced by the arrow cue and the feedback image (Tick = 'correct'; X mark = 'incorrect'). The arrow cue was constructed from two white line segments (line width = 0.11 dva) extending from the fixation point in one of the four diagonal directions. For arrows pointing to the near circles, each segment has a length of 0.32 dva and for arrows pointing to the far circles, each had a length of 0.65 dva. The target and the distractor were both black Landolt Cs (C-shaped rings). The inner Landolt-C was 1.14×1.14 dva, and the outer Landolt-C was approximately 1.32×1.32 dva (width \times height). Both Landolt-Cs were rotated

around their centers to face one of four cardinal directions (0°, 90°, 180°, or 270°). Stimulus opacity was adaptively adjusted using a Bayesian staircase (Watson & Pelli, 1983; Farell & Pelli, 1999) to maintain the accuracy on the task at 70% (PsychtoolBox QUEST algorithm, $\beta = 3.5$, $\Delta = 0.01$, $\gamma = 0.25$). Separate staircases were run for the inner and outer target locations.

Tagging Manipulation

In this study, Rapid Invisible Frequency Tagging (RIFT) was used to evoke a unique, frequency specific response that reflects visual processing of specific locations on the screen. To this end, a pair of diagonally opposite circles (randomly selected on each trial) was tagged until a response was recorded. This involved sinusoidally modulating the screen luminance at circle locations at a fixed frequency. Two frequencies (60Hz and 65.45Hz) were pseudo-randomly assigned to either the upper or the lower circle of the diagonal pair on each trial. The constructed sinusoids were always at the same phase at the moment of arrow cue onset. Temporal precision of the displayed stimuli was continually recorded using PsychToolBox's Screen('Flip') command. To account for any missed frames, an online correction was implemented that adjusted the phase of the tagging waveform forward to maintain its original phase trajectory when this command detected missed frames (mean = 17.72%, SD = 19.84%, median = 11.88% of trials). The mean number of missed frames per trial was 0.47 (SD = 2.94), with a median of 0.00, out of 1026 frames per trial after preprocessing.

Protocol

Participants took part in a 2-hour session conducted at the Division of Experimental Psychology, Utrecht University. Before the experiment sessions began, participants received procedural information and gave informed consent. On the informed consent sheet, they were asked to report their date of birth, biological sex, and dominant hand. Once the EEG setup was complete, participants were seated at a fixed distance of 56 cm from the monitor, with their chins positioned on a chinrest. The experiment was verbally explained using a visual guide. The participants were instructed to maintain a fixed gaze on the fixation cross in the center of the screen. Participants were also informed that they might occasionally notice visual artifacts or flickering on the screen and were later asked whether they did or not. They were also informed that the transparency of the targets might vary across trials. After receiving these instructions and completing a practice block of 15 trials, participants proceeded with the main experiment, which lasted approximately 50 to 60 minutes. Compensation was awarded either in cash or in participation credits (see **Participants**), and the session was ended.

Display Apparatus

Stimuli were presented on an LED-backlit LCD Alienware AW2524HF monitor (projected screen size: 54.5 × 30.5 cm (width × height)) (Dell Technologies, 2023), with a resolution of 1920 × 1080 pixels and a refresh rate of 360Hz. Experimental code was written using PsychToolBox (Brainard & Vision, 1997; Kleiner et al., 2007) in MATLAB (MATLAB, 2022).

EEG Recording and Pre-processing

EEG data was recorded using a 64-channel ActiveTwo BioSemi system (BioSemi B.V., Amsterdam, The Netherlands) at a sampling rate of 2048Hz. To monitor vertical and horizontal eye movements, two extra electrodes were positioned above the left eye and on the outer canthus. Just before the experiment began, signal quality across all channels was checked using BioSemi's ActiView software to ensure adequate recording quality. All data analysis was conducted using MATLAB's Fieldtrip Toolbox (Oostenveld et al., 2011). The EEG data was first re-referenced to the average of all channels (excluding poor channels, as determined by visual inspection, median = 13 channels per participant). The data was high-pass filtered (0.01Hz), then line noise and harmonics were removed using a DFT filter (50, 100, 150Hz). The data was segmented into trials ranging from 0.7 seconds before to 2.15 seconds after tagging onset. An ICA was performed to remove oculomotor artifacts, and trials with other motor artifacts (as per visual inspection) or highnoise were removed (mean = 16.26%, SD = 12.20%, median = 14.61% of trials)

RIFT Response: Coherence

Magnitude-squared coherence was used to determine the strength of the EEG response to RIFT frequencies of interest. Coherence is a dimensionless quantity ranging from 0 to 1 that quantifies the consistency of two signals in their frequency and phase alignment. High coherence values are achieved when two signals oscillate at the same frequency with a consistent phase difference across trials. Coherence was computed between a reference wave (pure sinusoids at the corresponding 60Hz/65.45Hz frequency, sampled at 2048Hz) for a set of trials per channel and participant. The 2.85s trials were first bandpass filtered (±1.9/2.5Hz) at the frequencies of interest (60Hz & 65.45Hz) using a two-pass Butterworth filter (4th order, Hamming taper). The filtered time-series data was Hilbert transformed. This yielded the instantaneous magnitude, $M_x(t)$, and phase, $\phi(t)$, of the bandpass-filtered EEG signal. To compute time-varying coherence, the following equation was used:

$$coh(t) = \frac{\left| \sum_{t=1}^{n} \vec{M}_{x}(t) \vec{M}_{y}(t) e^{i\Delta \vec{\phi}_{xy}(t)} \right|^{2}}{n \sum_{t=1}^{n} \vec{M}_{x}(t)^{2} \vec{M}_{y}(t)^{2}}$$

where $\vec{M}_x(t)$ and $\vec{M}_y(t)$ are the instantaneous magnitudes of the EEG signal and the reference sinusoid, respectively, and $\vec{\phi}_{xy}(t)$ is the difference between their instantaneous phases across all n trials. Coherence spectrograms were created to inspect the sharpness of the signal by calculating coherence across frequencies ranging from 57Hz to 67.5Hz in 0.5Hz intervals. We selected the top ten channels with the strongest coherence at 60 and 65.45Hz across all trials for each participant. Previous work (Arora et al., 2025) has shown that the number of selected channels has negligeable impact on relative coherence differences between experimental conditions. This top channel selection was repeated per condition (i.e., location-wise and attentional condition splits) for each participant for further analysis. All subsequent comparisons across experimental conditions were based on traces averaged across the top ten channels.

General Statistical Analysis

A cluster-based permutation test was used to compare condition-wise attentional differences in coherence over the course of each trial (Maris & Oostenveld, 2007). First, coherence traces were averaged over the ten channels with the strongest RIFT coherence at 60/65.45Hz for each participant, yielding a single coherence trace over time for each condition at each frequency. To investigate the differences across attentional conditions, the uncued condition trace was subtracted from the cued condition trace for each frequency and participant. We then applied a cluster permutation test to assess statistical significance (Maris & Oostenveld, 2007). A onesample t-test was performed at each individual time point on this difference trace to identify intervals that were significantly different from zero (p < 0.05). Clusters were defined as sequences of consecutive significant time points, and only those spanning at least 10ms were retained. For each cluster, a cluster-level test statistic was computed by summing the corresponding t-values (tmass). To construct a reference distribution under the null hypothesis, we randomly flipped the sign of each participant's difference trace to preserve temporal autocorrelations while removing consistent condition effects. This procedure was repeated 5000 times, and the maximum t-mass from each permutation was stored to form the reference distribution. Finally, we assessed whether the t-masses of any observed clusters exceeded 95% of the null distribution, and clusters exceeding this threshold were considered statistically significant. Coherence values were compared between cued versus uncued locations separately for each tagging frequency, and results were later averaged across frequencies for further analysis.

Results

Behavioral results from the experiment showed that participants performed the task successfully. The overall performance was above chance (mean = 72.48%, SD = 2.45%, median = 71.66%). Similarly, the performance on inner trials (mean = 71.27%, SD = 2.56%, median = 71.04%) and outer trials (mean = 73.76%, SD = 3.87%, median = 72.01%) was above chance,

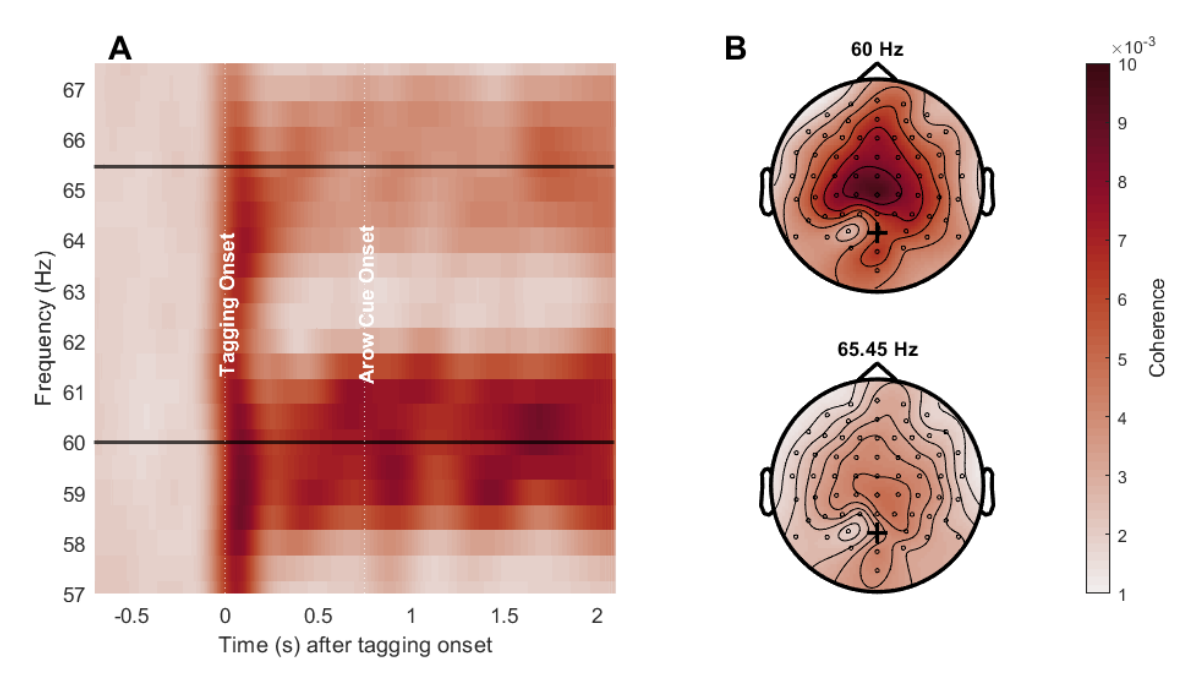


Figure 3.1 Average RIFT response (A) Coherence averaged across participants and top 10 channels with the highest coherence (selected individually per participant) showing clear peaks at 60 and 65.45Hz following flicker onset. The black horizontal lines are drawn at 60 and 65.45Hz. The vertical dashed lines indicate the tagging and cue onset. **(B)** Topographical distribution map of average RIFT coherence over the interval during which tagging manipulation was on. Black plus marks the POz electrode.

matching the staircase performance, which was set to target 70% accuracy (see **Stimuli**). All further analyses shown here were conducted using all trials (after preprocessing).

Tagging manipulation on Alienware AW2524HF monitor (refresh rate = 360Hz) evokes a RIFT response at the frequencies of interest

First, we verified that our tagging manipulation successfully evoked an oscillatory response in the EEG signal by computing coherence. Coherence from participants' top 10 channels showed a clear peak at the tagged frequencies 60 and 65.45Hz (**Figure 3.1.A**), demonstrating that we successfully captured two simultaneous RIFT-tags. In line with previous RIFT studies, the lower frequency (60Hz) flicker evoked a stronger response than the higher frequency (65.45Hz) flicker

as seen in both the spectrogram traces and the topographical maps (**Figure 3.1.A & 3.2.B**) as well as the time-resolved coherence traces (**Figure 3.2**). This was highest around central/parietal channels (**Figure 3.1.B**), unlike previous RIFT studies (Dimigen et al., 2025; Arora et al., 2025; Bouwkamp et al., 2025; Spaak et al., 2024; Zhigalov et al., 2019), where coherence is highest around parietal/occipital channels. We use the same color axis for 60 and 65.45Hz in **Figure 3.1.B** to allow for magnitude comparisons (but see **Figure S1** for a version with separate color bars for each frequency). The increase in coherence is aligned with the onset of the tagging manipulation period, and contrasts sharply with the baseline period without tagging (**Figure 3.1.A, Figure 3.2**). This confirms that the measured increase in coherence is directly caused by the tagging manipulation, and that the tagging worked as intended.

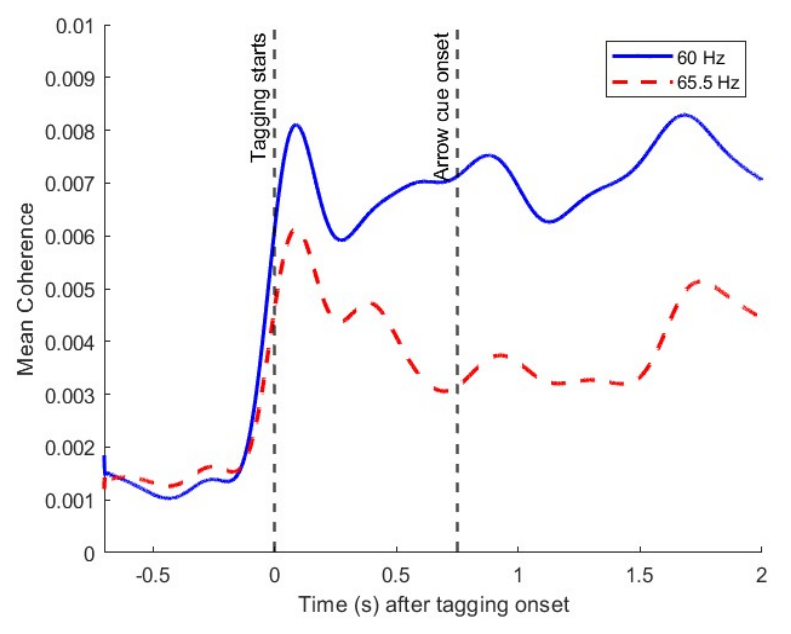


Figure 3.2: Time-resolved mean coherence traces for the 60 and 65.5Hz flickers. The blue trace represents the 60Hz coherence, and the red dashed trace represents the 65.45Hz coherence. Coherence values are averaged across the top ten channels exhibiting the highest overall RIFT response.

RIFT responses vary across different locations in the visual field

We investigated the extent to which RIFT responses differ for different locations in the visual field (see **Figure 2.1** for Task Design) to determine whether peripheral tagging regions evoked a clear RIFT response. The grand average coherence over the baseline tagging period (i.e., the period between tagging onset and arrow cue onset) suggests that the RIFT response is stronger for the lower visual field, and for locations at lower eccentricity (**Figure 3.3**). Here, the RIFT response, quantified using coherence, is averaged over the two tagging frequencies (i.e., 60 and 65.4Hz), with the same trend also observed for 60 and 65.45Hz separately (**Figure S2**).

To further investigate the RIFT signal at each tagging location, we provide spectrograms for each location condition (see **Figure 3.4**). These spectrograms show that although the RIFT

response decreases in magnitude with increasing eccentricity, a measurable signal is still present even at peripheral condition locations, irrespective of vertical/horizontal meridian, at 60 Hz. At 65.5 Hz, a response is also present, but much weaker in magnitude.

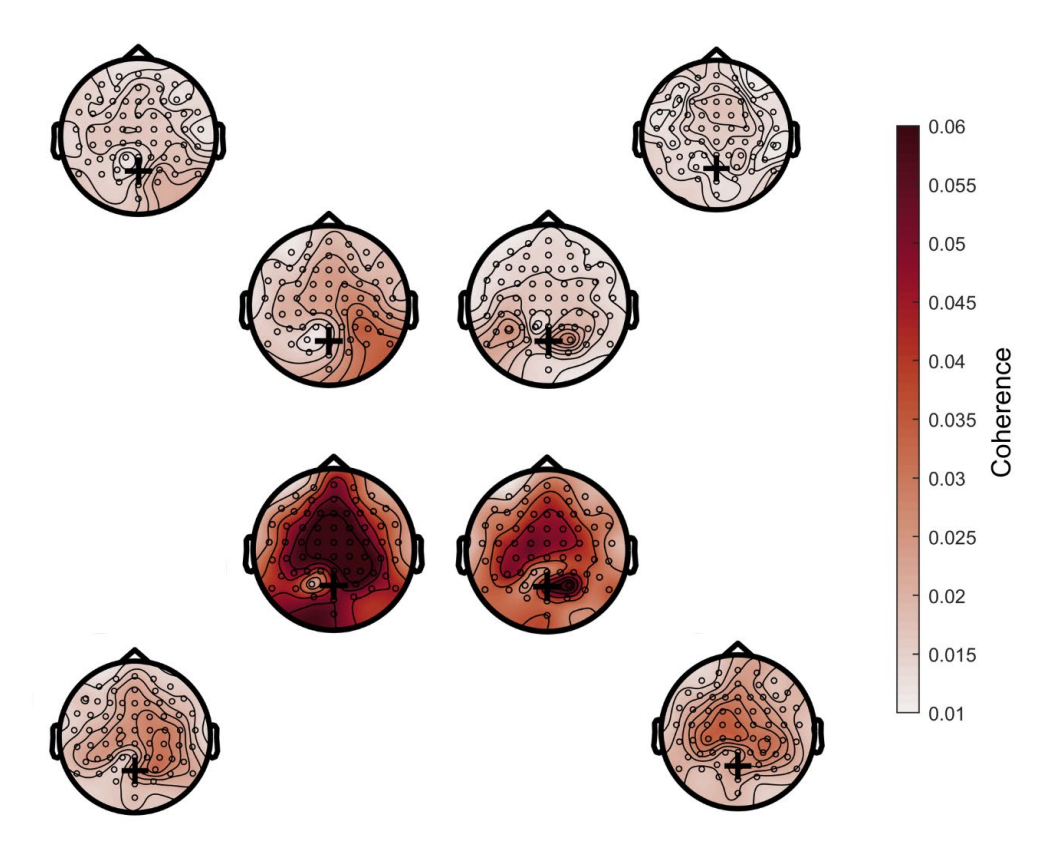


Figure 3.3: Average RIFT response by tagging location. Topographical distribution of average RIFT coherence during the baseline tagging interval, averaged over 60 and 65.45Hz. Topographies are positioned according to arrangement of tagging locations in the experimental display (see Figure 2.1). Black plus marks the POz electrode.

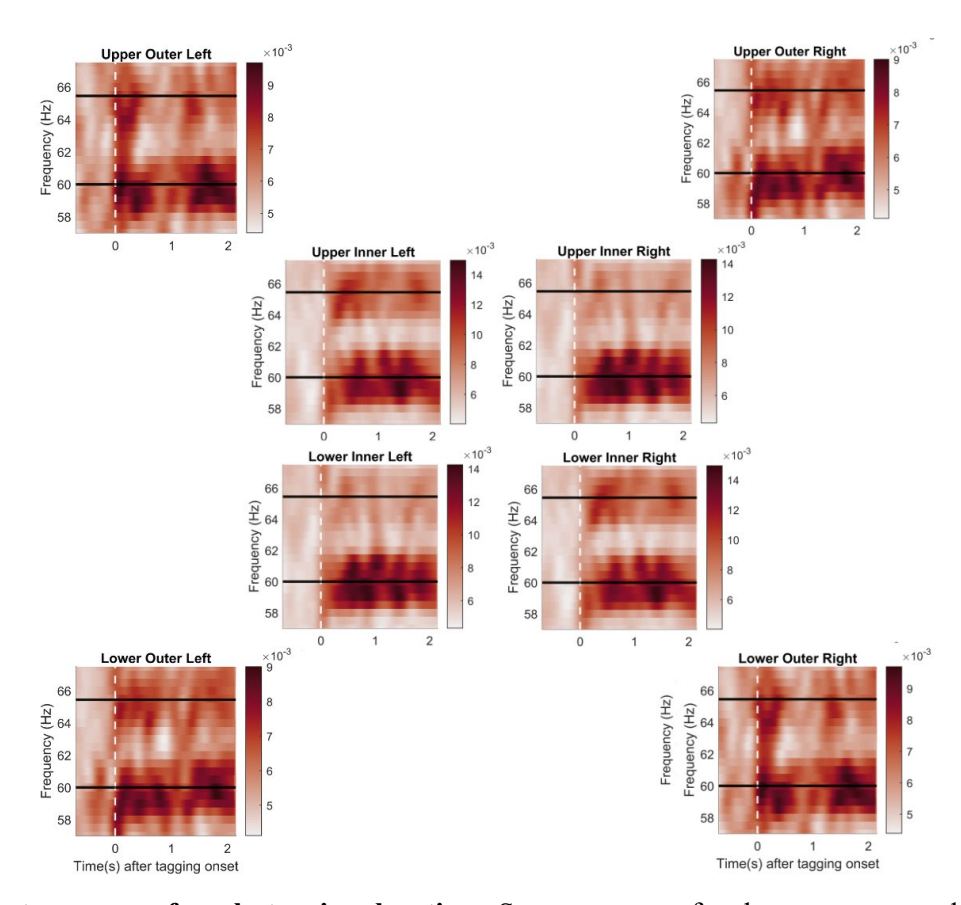


Figure 3.4: Spectrograms of each tagging location. Spectrograms of coherence averaged across participants at each location condition. Topographies are positioned according to arrangement of tagging locations in the experimental display (see Figure 2.1). The black horizontal lines are drawn at 60 and 65.45Hz. The vertical dashed line indicates the tagging onset.

Attention modulates the RIFT Response

We compared coherence traces (60 and 65.45Hz averaged) between cued and uncued locations to investigate attentional modulations of the RIFT response (**Figure 3.5**). For this, we used the 10 channels with the strongest coherence response per participant (See **RIFT Response: Coherence**). A clear difference in coherence was observed between cued and uncued locations, with the cued location showing a higher coherence than the uncued location. To quantify variability across participants, we computed 95% bootstrapped confidence intervals around the mean difference at each time point (based on n=5000 bootstrap samples). These intervals are shown as a shaded region around the difference trace. A cluster permutation test (red line in **Figure 3.5**) indicated a significant difference between cued and uncued item locations around 500 ms after cue onset (p = 0.0002; cluster extent ~0.5 s to ~1.3 s). This demonstrates that a RIFT-monitor setup can measure attentional modulations of the RIFT response before (during the spatial attentional shift) and after the appearance of the target stimulus.

The topographical distribution of the average difference in RIFT coherence between cued and uncued item locations, collapsed across both flicker frequencies and averaged over the significant interval (0.52–1.34s), shows a positive effect over occipital channels (**Figure 3.6**). Though this spatial distribution of attentional modulations is a marked shift from the overall coherence topographies (**Figure 3.1.B**) as it shows a more posterior distribution, it aligns with previous RIFT work (Arora et al., 2025; Dietz et al., 2025).

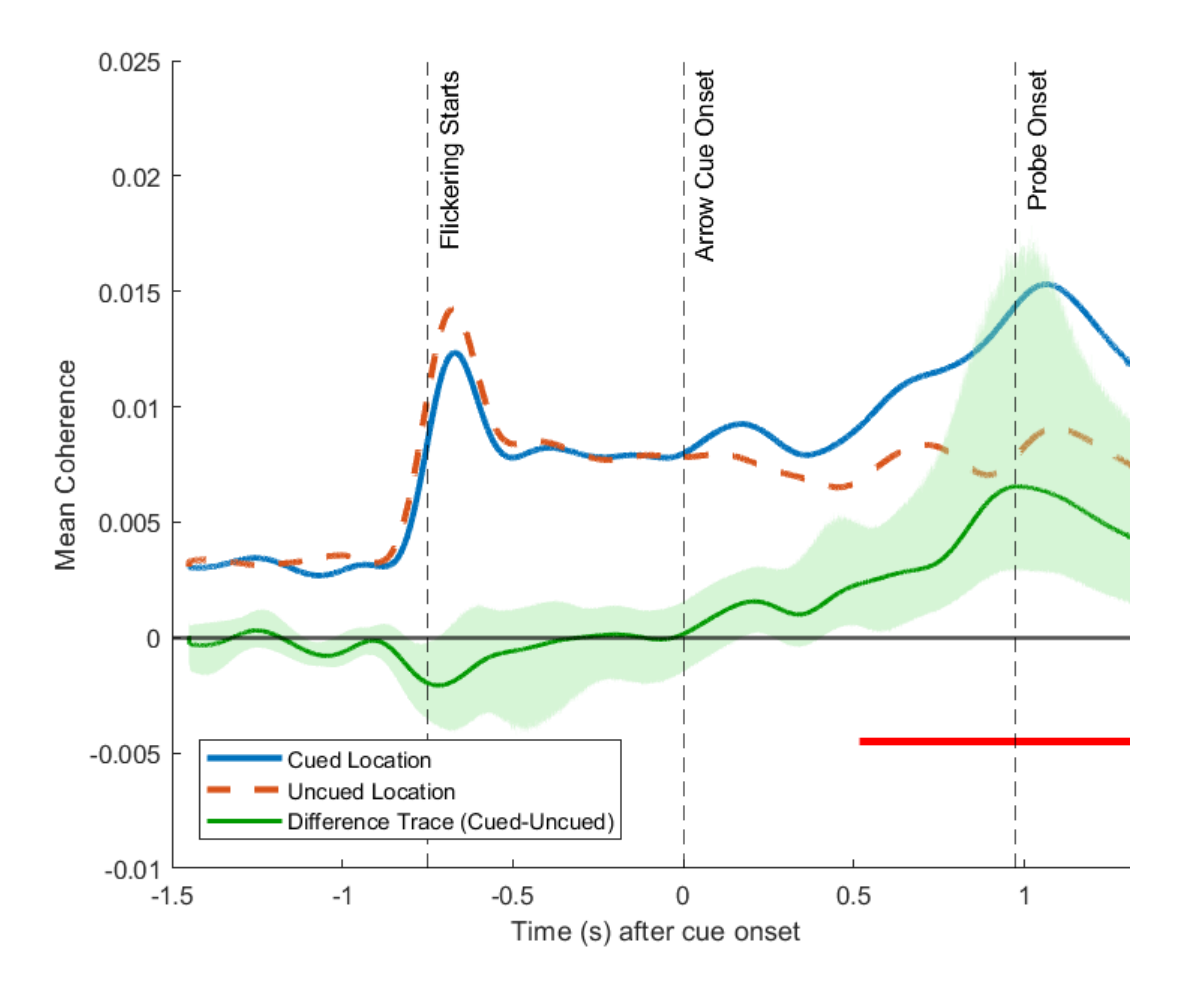


Figure 3.5: Average RIFT coherence at cued versus uncued locations. Coherence traces reflect signals from locations corresponding to cued (blue) and uncued (red dashed) stimuli, and their difference is given as the difference trace (green). The red line marks the time interval in which the cluster-based permutation test was significant. The vertical lines represent the tagging, arrow, and probe onset, respectively. The probe onset is marked at the midpoint between the minimum and maximum delays (0.85s –1.1s) following the arrow cue offset.

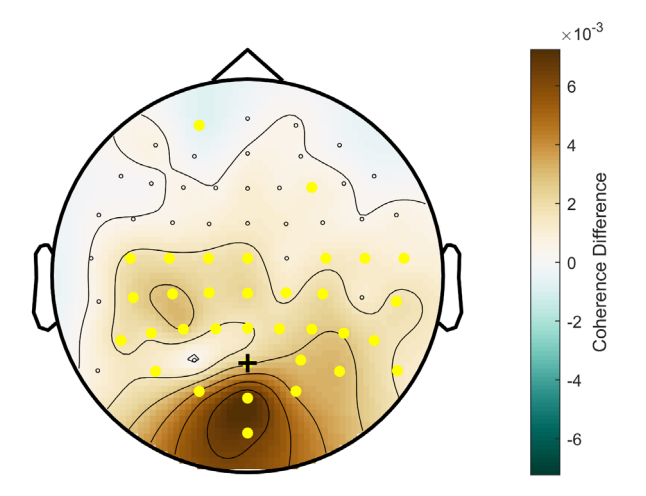


Figure 3.6: Topographical distribution of the difference between tagging responses from the cued and uncued locations. Average difference between coherence from cued and uncued item locations (averaged across all tagging positions, and over the interval 0.52-1.34s significant at the group level).

Attentional modulation across visual field locations

Lastly, we compared the attentional modulations to the RIFT response (60Hz and 65.45Hz averaged) elicited from cued versus uncued locations across the eight spatial location conditions separately. Since certain locations had a higher baseline tagging response, we eliminated the effects of overall magnitude differences by looking at relative (attentional modulation/baseline coherence over the tagging interval) effects. Topographical maps of the mean coherence difference between cued and uncued locations (**Figure 3.7**) suggest stronger attentional modulation of the RIFT signal at more foveal locations. Visual inspection of the topographies also suggests that the relative attentional modulation occurs predominantly in occipital regions and is relatively invariant to the retinal location of the tagged stimulus.

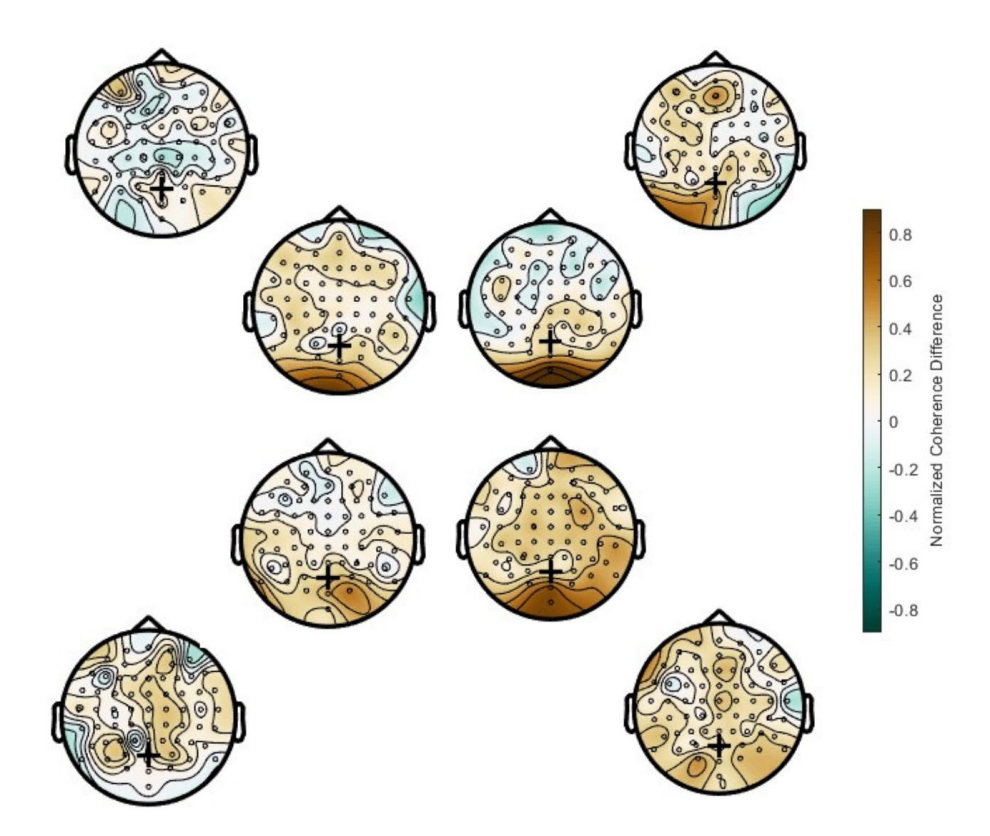


Figure 3.7: Location-wise differences between responses from cued and uncued tags. Topographical distributions of the mean coherence difference between cued and uncued locations for each of the eight spatial location conditions, averaged across flicker frequencies and the interval significant at the group level (0.52–1.34s).

Discussion

This study implemented Rapid Invisible Frequency Tagging (RIFT) along with an attentional cueing task on a 360Hz refresh rate consumer-grade monitor. We show that attentional modulations to the RIFT response can be captured on a monitor-based display setup. Our findings present an essential extension to recent work by Dimigen et al. (2025), who showed that a 480Hz refresh rate monitor can be used to evoke RIFT responses at 60Hz and 64Hz, however, without testing if these responses are modulated by attention. This is a notable advancement in the field of RIFT, as all existing RIFT research prior to this has utilized the PROPixx projector, which is a relatively expensive piece of specialized display hardware (~30x the cost of the monitor used here). We show here that a similar monitor setup (Alienware Gaming Monitor AW2524HF at 360Hz refresh) can produce frequency-specific neural responses at 60 and 65.45Hz and, more importantly, that it can measure modulations to these tagging responses by covert attention via a simple cueing paradigm.

We show that upon cueing participants to a location on the screen for the report of an upcoming probe, the tagging response is significantly higher for cued as compared to uncued locations. This attentional modulation can already be observed prior to probe onset. Thus, we show that even on a consumer-grade display setup, the RIFT response is sensitive enough to capture modulations to early visual processing induced by covert shifts of attention. We also noted that the topographical distribution of these modulations originated predominantly from occipital electrodes and was relatively invariant to the location of the tagged stimulus. This was the case even though tagging in the lower visual field evoked a far stronger overall RIFT response, as has been seen previously (Minarik et al., 2023). This suggests that visual asymmetries in the overall RIFT response may not be a concern when it comes to measuring attentional modulations to this response.

Although prior RIFT-monitor work measured very weak tagging responses when tagging peripherally (Dimigen et al., 2025), we show here that peripheral tagging on a monitor is both reliably observable as well as sensitive enough to pick up on attentional modulations. However, it is worth noting that our tagging was less eccentric (4.5 dva and 8.1 dva) than the peripheral tagging in Dimigen et al. (2025) (12 dva), which is the likely cause of the difference in tagging strength.

A key consideration in RIFT experimentation is the invisibility of the tagging. Since this is generally assumed to be a function of refresh rate (i.e., higher refresh rates are less susceptible to visibility of the tagging), this is a key concern with monitor setups such as the 360Hz setup used here as compared to the 1440Hz refresh rate of the PROPixx projector. Although no participant perceived the flicker continuously, they all reported being aware of some screen changes - likely the visual glitches on the screen caused by missed frames. Though we did not empirically test for tagging visibility here, these reports are similar to those of Dimigen et al. (2025). Further research

should be conducted to verify whether this monitor setup reliably achieves invisible frequency tagging before using it to tag locations that are perceptually indistinguishable from background space, where the flicker is more susceptible to being visible. However, when tagging stimuli with clearly defined boundaries or outlines, as was the case here, RIFT implementations paired with monitor setups appear to be promising low-cost alternatives to using expensive projectors.

These findings offer sufficient evidence in support of a 360Hz refresh-rate consumer-grade monitor as a display apparatus compatible with RIFT, forming a far more affordable alternative to the projector setups traditionally used in RIFT research. Our results show that RIFT with a monitor implementation can successfully capture neural responses to multiple rapidly flickering stimuli, as well as modulations to these responses by covert spatial attention. By doing so, we demonstrate that consumer grade monitors are a valid choice for implementing invisible frequency tagging. We hope that this study will serve as a basis for future RIFT research (e.g., on spatial attention) using consumer-grade high-refresh-rate gaming monitors and facilitate its widespread application.

References

- Abrams, J., Nizam, A., & Carrasco, M. (2012). Isoeccentric locations are not equivalent: the extent of the vertical meridian asymmetry. Vision research, 52(1), 70–78. https://doi.org/10.1016/j.visres.2011.10.016
- Anton-Erxleben, K., & Carrasco, M. (2013). Attentional enhancement of spatial resolution: linking behavioural and neurophysiological evidence. Nature Reviews Neuroscience, 14(3), 188-200.
- Arora, K., Gayet, S., Kenemans, J. L., Van der Stigchel, S., & Chota, S. (2024). Using Rapid Invisible Frequency Tagging to track internal attention. Journal of Vision, 24(10), 603-603.
- Arora, K., Gayet, S., Kenemans, J. L., Van der Stigchel, S., & Chota, S. (2025). Dissociating external and internal attentional selection. iScience, 28(4).
- Benson, N. C., Kupers, E. R., Barbot, A., Carrasco, M., & Winawer, J. (2021). Cortical magnification in human visual cortex parallels task performance around the visual field. Elife, 10, e67685.
- Bouwkamp, F. G., de Lange, F. P., & Spaak, E. (2025). Spatial predictive context speeds up visual search by biasing local attentional competition. Journal of Cognitive Neuroscience, 37(1), 28-42.
- Boynton, G. M. (2009). A framework for describing the effects of attention on visual responses. Vision research, 49(10), 1129-1143.
- Brown H., Eley T., Broeren S., MacLeod C., Rinck M., Hadwin J., Lester K. Psychometric properties of reaction time based experimental paradigms measuring anxiety-related information-processing biases in children. J. Anxiety Disord. 2014;28(1):97–107. doi: 10.1016/j.janxdis.2013.11.004.
- Croner, L. J., & Kaplan, E. (1995). Receptive fields of P and M ganglion cells across the primate retina. Vision research, 35(1), 7-24.
- Curcio, C. A., & Allen, K. A. (1990). Topography of ganglion cells in human retina. Journal of comparative Neurology, 300(1), 5-25.
- Danckert, J. A., Goodale, M. A., & Johnson-Frey, S. H. (2003). Taking action: Cognitive neuroscience perspectives on intentional acts. Ups and downs in the visual control of action, 29-64.
 - Dell Technologies. (2023). Alienware 25 Gaming Monitor AW2524HF.

- Dietz, L., Strauch, C., Arora, K., Van der Stigchel, S., Chota, S., & Gayet, S. (2025). Anticipated relevance prepares visual processing for efficient memory-guided selection. bioRxiv, 2025-08.
- Dimigen, O., & Stein, A. (2024). A high-speed OLED monitor for precise stimulation in vision, eye-tracking, and EEG research. bioRxiv, 2024-09.
- Drijvers, L., Jensen, O., & Spaak, E. (2021). Rapid invisible frequency tagging reveals nonlinear integration of auditory and visual information. Human Brain Mapping, 42(4), 1138-1152.
- Duecker, K., Gutteling, T. P., Herrmann, C. S., & Jensen, O. (2021). No evidence for entrainment: endogenous gamma oscillations and rhythmic flicker responses coexist in visual cortex. Journal of Neuroscience, 41(31), 6684-6698.
- Duecker, K., Shapiro, K. L., Hanslmayr, S., Griffiths, B. J., Pan, Y., Wolfe, J., & Jensen, O. (2024). Guided visual search is associated with a feature-based priority map in early visual cortex. bioRxiv, 2024-10.
- Farell, B., & Pelli, D. G. (1999). Psychophysical methods, or how to measure a threshold and why. Vision research: A practical guide to laboratory methods, 5, 129-136.
- Gordon, J., Shapley, R., Patel, P., Pastagia, J., & Truong, C. (1997, March). The lower visual field is better than the upper visual field at red/green recognition. In INVESTIGATIVE OPHTHALMOLOGY & VISUAL SCIENCE (Vol. 38, No. 4, pp. 4199-4199). 227 EAST WASHINGTON SQ, PHILADELPHIA, PA 19106: LIPPINCOTT-RAVEN PUBL.
- He, S., Cavanagh, P., & Intriligator, J. (1996). Attentional resolution and the locus of visual awareness. Nature, 383(6598), 334-337.
- Heitmann, C., Zhan, M., Linke, M., Hölig, C., Kekunnaya, R., van Hoof, R., Goebel, R., & Röder, B. (2023). Early visual experience refines the retinotopic organization within and across visual cortical regions. Current biology: CB, 33(22), 4950–4959.e4. https://doi.org/10.1016/j.cub.2023.10.010
- Herrmann, C. S. (2001). Human EEG responses to 1–100 Hz flicker: resonance phenomena in visual cortex and their potential correlation to cognitive phenomena. Experimental brain research, 137, 346-353.
- Hustá, C., Meyer, A., & Drijvers, L. (2025). Using rapid invisible frequency tagging (RIFT) to probe the neural interaction between representations of speech planning and comprehension. Neurobiology of Language, 1-36.

- Intriligator, J., & Cavanagh, P. (2001). The spatial resolution of visual attention. Cognitive psychology, 43(3), 171-216.
- Jóhannesson, Ó. I., Tagu, J., & Kristjánsson, Á. (2018). Asymmetries of the visual system and their influence on visual performance and oculomotor dynamics. European Journal of Neuroscience, 48(11), 3426-3445.
- Kraft, A., Sommer, W. H., Schmidt, S., & Brandt, S. A. (2011). Dynamic upper and lower visual field preferences within the human dorsal frontoparietal attention network. Human brain mapping, 32(7), 1036-1049.
- Kravitz, D. J., Saleem, K. S., Baker, C. I., & Mishkin, M. (2011). A new neural framework for visuospatial processing. Nature Reviews Neuroscience, 12(4), 217-230.
- Kulke, L. V., Atkinson, J., & Braddick, O. (2016). Neural differences between covert and overt attention studied using EEG with simultaneous remote eye tracking. Frontiers in human neuroscience, 10, 592.
- Levine, M. W., & McAnany, J. J. (2005). The relative capabilities of the upper and lower visual hemifields. Vision research, 45(21), 2820-2830.
- Maris, E., and Oostenveld, R. (2007). Nonparametric statistical testing of EEG-and MEG-data. J. Neurosci. Methods 164, 177–190.
- Minarik, T., Berger, B., & Jensen, O. (2023). Optimal parameters for rapid (invisible) frequency tagging using MEG. NeuroImage, 281, 120389.
- Morgan, S., Hansen, J., & Hillyard, S. (1996). Selective attention to stimulus location modulates the steady-state visual evoked potential. Proceedings of the National Academy of Sciences, 93(10), 4770–4774.
- Müller, M. M., & Hillyard, S. (2000). Concurrent recording of steady-state and transient event-related potentials as indices of visual-spatial selective attention. Clinical Neurophysiology, 111(9), 1544-1552.
- Müller, M. M., & Hübner, R. (2002). Can the spotlight of attention be shaped like a doughnut? evidence from steady-state visual evoked potentials. Psychological science, 13(2), 119–124.
- Noudoost, B., Chang, M. H., Steinmetz, N. A., & Moore, T. (2010). Top-down control of visual attention. Current opinion in neurobiology, 20(2), 183-190.

- Oostenveld, R., Fries, P., Maris, E., & Schoffelen, J. M. (2011). FieldTrip: open source software for advanced analysis of MEG, EEG, and invasive electrophysiological data. Computational intelligence and neuroscience, 2011(1), 156869.
- Pan, W. N., Zhao, Y. W., Luo, Z. X., Chen, Y., & Cai, Y. C. (2024). Attention modulates early visual processing: An association between subjective contrast perception and early C1 ERP component. Psychophysiology, 61(5), e14507.
- Pan, Y., Frisson, S., & Jensen, O. (2021). Neural evidence for lexical parafoveal processing. Nature Communications, 12(1), 5234.
- Regan, D. (1966). An effect of stimulus colour on average steady-state potentials evoked in man. Nature, 210(5040), 1056-1057.
- Rossit, S., McAdam, T., Mclean, D. A., Goodale, M. A., & Culham, J. C. (2013). fMRI reveals a lower visual field preference for hand actions in human superior parieto-occipital cortex (SPOC) and precuneus. Cortex, 49(9), 2525-2541.
- Schmidtmann, G., Logan, A. J., Kennedy, G. J., Gordon, G. E., & Loffler, G. (2015). Distinct lower visual field preference for object shape. Journal of Vision, 15(5), 18-18.
- Seijdel, N., Marshall, T. R., & Drijvers, L. (2023). Rapid invisible frequency tagging (RIFT): a promising technique to study neural and cognitive processing using naturalistic paradigms. Cerebral Cortex, 33(5), 1626-1629.
- Serrien, D. J., & O'Regan, L. (2025). Word perception and upper-lower visual field asymmetries. Brain and Cognition, 186, 106294.
- Spaak, E., Bouwkamp, F. G., & de Lange, F. P. (2024). Perceptual foundation and extension to phase tagging for rapid invisible frequency tagging (RIFT). Imaging Neuroscience, 2, 1-14.
- Thai, N., Taber-Thomas, B. C., & Pérez-Edgar, K. E. (2016). Neural correlates of attention biases, behavioral inhibition, and social anxiety in children: An ERP study. Developmental cognitive neuroscience, 19, 200-210.
- Watson, A. B., & Pelli, D. G. (1983). QUEST: A Bayesian adaptive psychometric method. Perception & Psychophysics, 33(2), 113–120. https://doi.org/10.3758/BF03202828
- Wertheim, T. H., & DUNSKY, I. L. (1980). Peripheral visual acuity. Optometry and Vision Science, 57(12), 915-924.

Woertz, E. N., Wilk, M. A., Duwell, E. J., Mathis, J. R., Carroll, J., & DeYoe, E. A. (2020). The relationship between retinal cone density and cortical magnification in human albinism. Journal of Vision, 20(6), 10-10.

Zhigalov, A., Herring, J. D., Herpers, J., Bergmann, T. O., & Jensen, O. (2019). Probing cortical excitability using rapid frequency tagging. NeuroImage, 195, 59-66.

Appendix

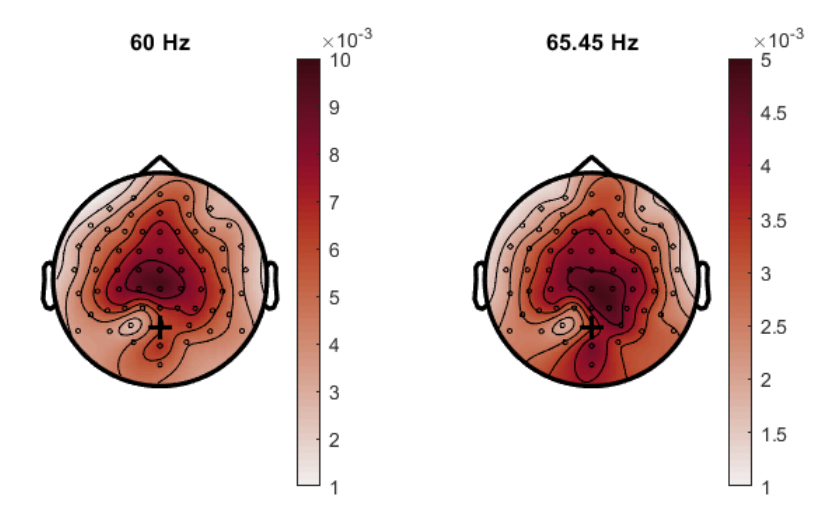


Figure S1: Topographies of the average RIFT response per frequency using separate y-axis limits. Topographical distribution map of average RIFT coherence over the interval during which tagging manipulation was on. Separate y-axis (color scale) limits were used for the two frequencies of interest to enhance the visibility of spatial detail, particularly for the 65.45Hz response (which was not clearly visible in Figure 3.1.B).

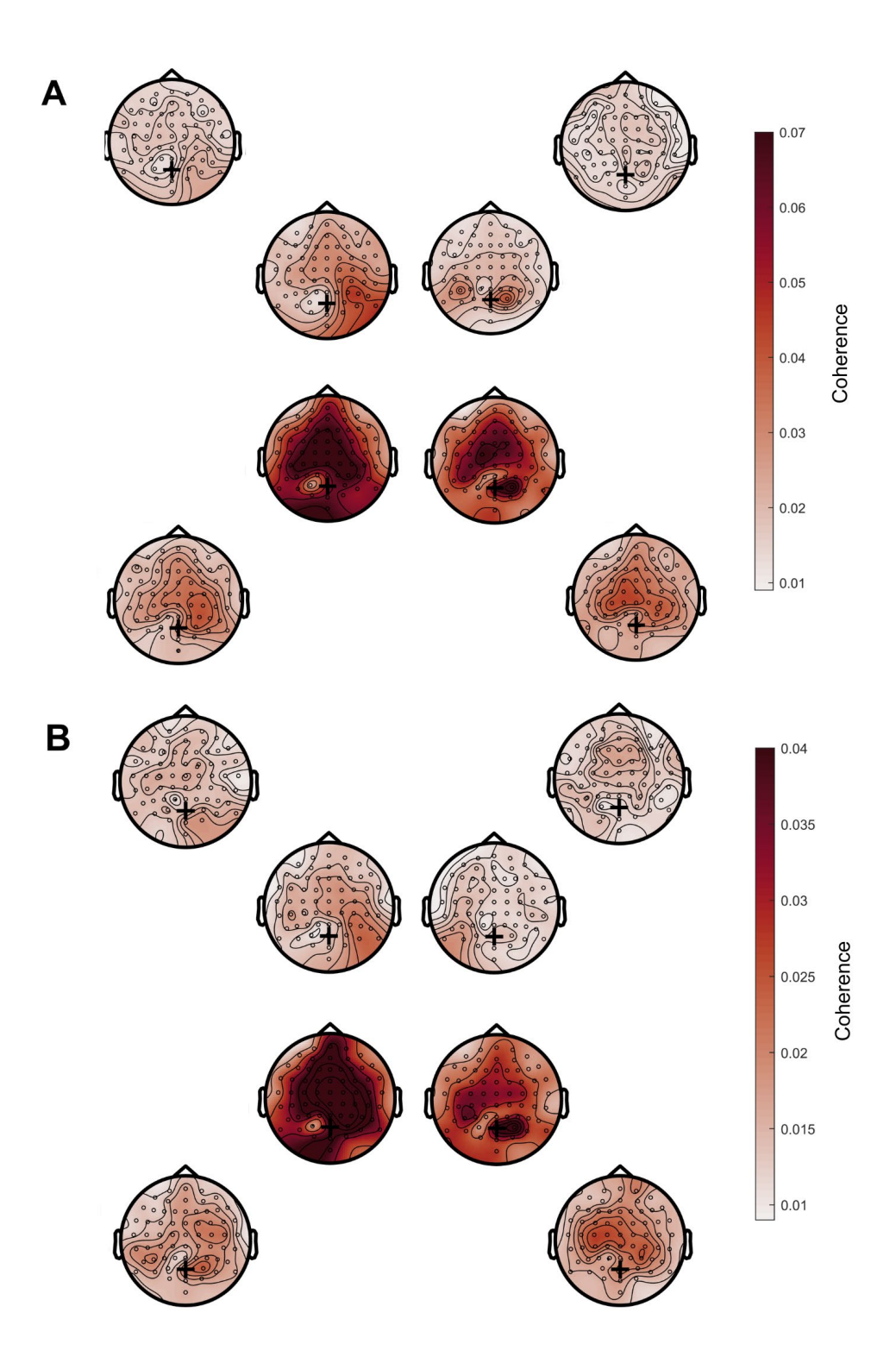


Figure S2: RIFT response per location condition at 60 and 65.45Hz separately. Topographical distribution of RIFT coherence during the baseline tagging interval at 60Hz (A) and 65.45Hz (B). Black plus marks the POz electrode. Participant 10 is excluded from this visualisation for clarity and interpretability.